Effects of He^+ Implantation on the Surface Morphology of SiC

S.J. Zenobia, G.L. Kulcinski, R.F. Radel,
D.R. Boris, R.P. Ashley

November 2006

UWFDM-1339

Prepared for the 17th ANS Topical Meeting on Fusion Energy, 13-15 November 2006, Albuquerque NM.

FUSION TECHNOLOGY INSTITUTE

UNIVERSITY OF WISCONSIN

MADISON WISCONSIN

Effects of He^+ Implantation on the Surface Morphology of SiC

S.J. Zenobia, G.L. Kulcinski, R.F. Radel, D.R. Boris, R.P. Ashley

Fusion Technology Institute
University of Wisconsin
1500 Engineering Drive
Madison, WI 53706

http://fti.neep.wisc.edu

November 2006

UWFDM-1339

Prepared for the 17th ANS Topical Meeting on Fusion Energy, 13-15 November 2006, Albuquerque NM.

Effects of He^+ Implantation on the Surface Morphology of SiC

S.J. Zenobia, G.L. Kulcinski, R.F. Radel, D.R. Boris, R.P. Ashley

Fusion Technology Institute, 1500 Engineering Drive, Madison, WI 53706 zenobia@wisc.edu

Abstract: *Candidate materials for the first wall armor of the HAPL chamber must be able to withstand temperatures near their operational limit and significant radiation damage due to ion bombardment. The resilience of silicon carbide (SiC) to these conditions has been investigated using energetic helium ions to simulate Inertial Confinement Fusion (ICF) target debris.*
SiC samples were irradiated to 10^{19} He^+/cm^2 and 750 – 1150°C. Scanning electron microscope (SEM) analysis indicates significant surface blistering and flaking, with the severity corresponding to the temperature and fluence of the samples. SiC samples have also been irradiated to fluences of 10^{18} He^+/cm^2 at 750 and 950°C and 10^{19} He^+/cm^2 at 950°C. These samples also appear to indicate extensive surface blistering and flaking. Sample irradiation was performed in the Inertial Electrostatic Confinement (IEC) facility at the University of Wisconsin-Madison and damage analysis was performed with a LEO 1530 SEM.

I. INTRODUCTION

The viability of any commercial fusion reactor, whether using magnetically or inertially confined plasmas, depends on the lifetime of the containment vessel. Most often the extension of this lifetime to practical operation times is a materials issue. More specifically, the ability of the first wall armor of these devices to absorb severe radiation fluxes and maintain their integrity is crucial. This research focuses on the first wall armor of the proposed HAPL chamber, which will experience substantial light ion fluxes ranging in energy from ~10 keV to several MeV. The UW IEC device simulates the lower portion of the HAPL energy spectrum.[1] Previous work has focused on refractory metals, alloys, and metallic foams. Some examples are tungsten, tungsten-rhenium alloy, and hafnium and tantalum carbide foams.[2]

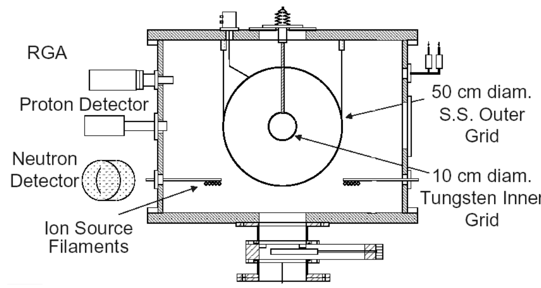

Figure 1. UW-IEC Device

II. OPERATION OF THE UW-IEC DEVICE

The UW IEC experiment focuses on the uses of inertial electrostatic fusion for various applications.[3] One of these applications is the simulation of ion damage to both fission and fusion materials at high temperatures. These materials are bombarded with D^+ and He^+ using the UW IEC device. A schematic of the IEC device is shown in Figure 1. The aluminum vacuum chamber is 65 cm tall with a 90 cm diameter. Base pressure is kept at ~10^{-5} Pa (10^{-7} torr) using a turbo pump. Normal operation consists of two highly transparent concentric grids suspended in the vacuum chamber. The outer stainless steel grid (diameter = 50 cm) is an anode held at ground potential, while the inner tungsten rhenium grid (diameter = 10 cm) is the cathode placed at a negative potential ranging from 0 – 200 kV. Cathode voltages are attained from the 200 kV power supply connected by a high voltage feedthrough.

Nominally, a background pressure ~0.3 Pa (2 mtorr) of deuterium or helium fuel gas is fed into the vacuum chamber and ionized by electron bombardment produced by light bulb filaments. The positively charged ions are attracted to the cathode's negative potential and spherically converge in the center of the grid, resulting in fusion reactions.

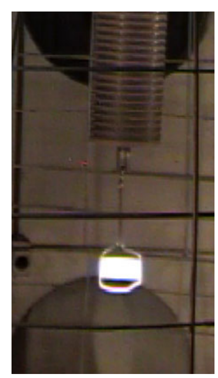

Figure 2. SiC During Irradiation

To irradiate these materials the inner grid is replaced by a tungsten rhenium mount which holds the sample via tension or a spot weld. An example is shown in Figure 2. The background fuel gas pressure is reduced to ~0.7 Pa (0.5 mTorr) and supply voltages range from 20 – 30 kV. This decrease in background pressure is to facilitate a more uniform energy distribution of the D^+ or He^+.

III. SETUP AND EXPERIMENTAL PROCEDURE

III.A. CVD SiC Pre-irradiation

As received CVD SiC samples were acquired from Dr. Lance Snead at ORNL and are shown in Figure 3 below. The samples, as received, are 2.5 cm by 0.6 cm. SEM micrographs were taken of the mirror finished side of the SiC before and after irradiation. Figure 4 is an SEM image of pre-irradiated SiC. Surface defects on the virgin sample appear to ~ 0.1 microns or less.

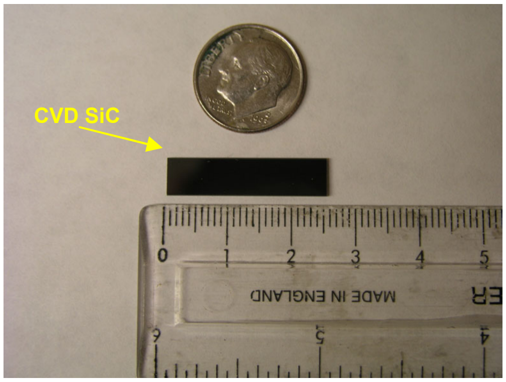

Figure 3. As Received CVD SiC

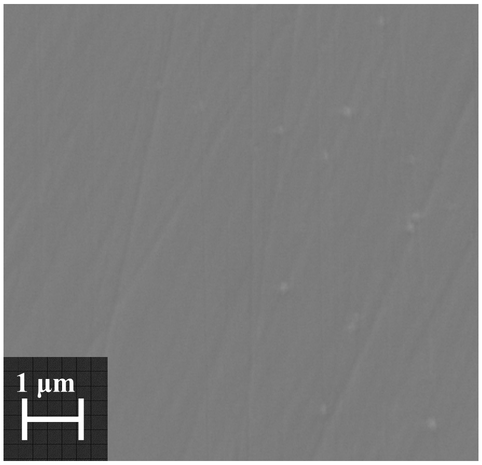

Figure 4. Unirradiated SiC

III.B. Calculation of Irradiation Parameters

SRIM[4] calculations were performed to estimate the range of He^+ in SiC implanted by the IEC device. The calculation modeled the SiC by a homogenous and equal ratio of silicon and carbon. Calculations were done for typical IEC He^+ implantation energies (20, 30, and 40 keV). Figure 5 shows the calculated ion concentration [atoms/cm^3] as a function of depth in the SiC. In Figure 6 the depth of the peak He^+ concentration is plotted against the ion implantation energies using the results presented in Figure 5.

After pre-irradiation analysis with the SEM, CVD SiC samples were irradiated to temperatures between 750°C and 950°C and fluences of 1×10^{18} He^+/cm^2 and 1×10^{19} He^+/cm^2. The temperatures were measured using a two-color infrared pyrometer. Table 1 shows a summary of these irradiation experiments. Irradiation times ranged from approximately 10 minutes to 2 ½ hours, depending on the desired fluence and irradiation temperature desired for each sample. The current and voltage (ion energy) were constantly monitored to ensure constant ion flux over the irradiation period.

IV. RESULTS AND DISCUSSION

For each of the samples irradiated scanning analysis was performed using an SEM. These micrographs illustrate the adverse effects on CVD SiC surface morphology under helium ion bombardment.

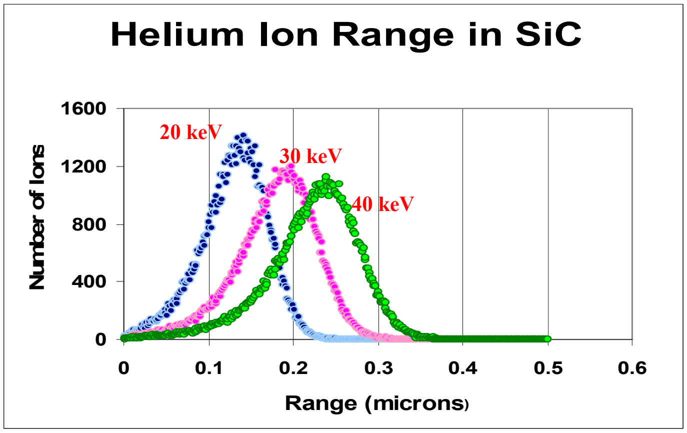

Figure 5. SRIM Calculates the Range of IEC He^+ in SiC for Relevant Implantation Energies

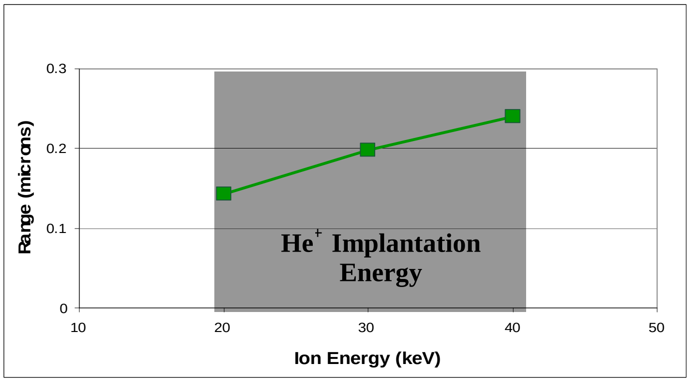

Figure 6. The Depth of Peak He^+ Concentrations are Plotted for Each of the Implantation Energies

IV.A. Irradiation to $1\text{x}10^{19}$ He^+/cm^2 at 750 – 950 °C

Three SiC samples were irradiated to $1\text{x}10^{19}$ He^+/cm^2 at temperatures of 750, 850, and 950 °C. At a constant fluence, increasing the irradiation caused an increase in the depth of the cratering and dimpling observed on the SiC surface. At 950 °C, pore formation on the SiC surface became the dominant form of damage over the cratering, while extensive flaking was observed at 850 °C. One also notices that the damage is inhomogeneous over the sample surface. The SEM micrographs from this constant fluence temperature scan are shown in Figure 7.

Table 1. Summary of Irradiation Experiments

Sample	Temperature °C	Fluence He^+/cm^2	Ion Energy keV
SiC3a	950	1018	30
SiC3b	950	1019	35
SiC4a	750	1018	20
SiC4b	850	1018	30
SiC5 (mask)	950	1019	30
SiC6a	750	1019	30
SiC6b	850	1019	30

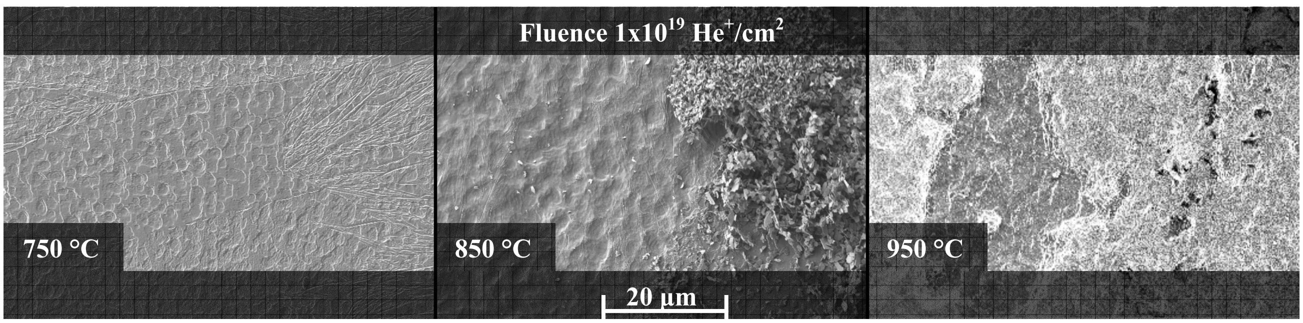

Figure 7. Temperature Scan at 10^{19} He^+/cm^2

IV.B. Irradiation at Constant Temperature and Varying Fluence

Irradiations to examine damage as a function of fluence at a constant temperature were also performed. Two SiC samples were irradiated at 750 °C to fluences of 10^{18} and 10^{19} He^+/cm^2 (see Figure 8). The sample irradiated to 10^{18} He^+/cm^2 exhibits flaking and minor pore formation, while the sample with higher fluence has not sustained this flaking or pore formation. In fact, the cratering is the dominant effect in the higher fluence sample at this temperature. The reason for this response is currently not understood. The samples irradiated at 850 ºC and fluences of 10^{18} and 10^{19} He^+/cm^2 both incurred substantial damage to the surface morphology. Flaking is the dominant form of damage observed in these samples with pore formation as an auxiliary damage mechanism. An important observation from Figure 9 below is the congregations or "lakes" of flaked SiC located on the sample surface. Secondly, the thickness of these flakes roughly corresponds to the predicted helium ion range from SRIM calculations for these implantation energies.

A set of samples was irradiated at 950 °C and fluences of 10^{18} and 10^{19} He^+/cm^2. The set of SEM images in Figure 10 reveals that while flaking occurs on the lower fluence specimen, there is an increase in pore formation. The higher fluence sample shows that pore formation is the primary damage mechanism and there are large pitted areas across the sample. These areas

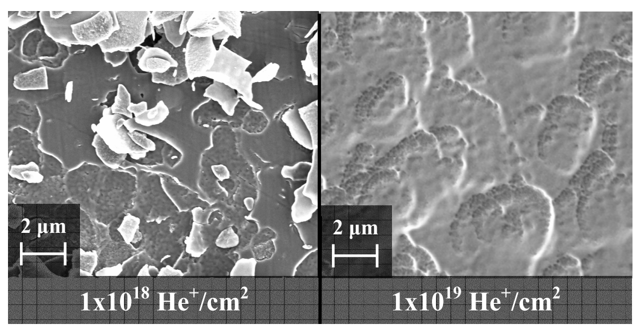

Figure 8. SiC Irradiated at 750 °C

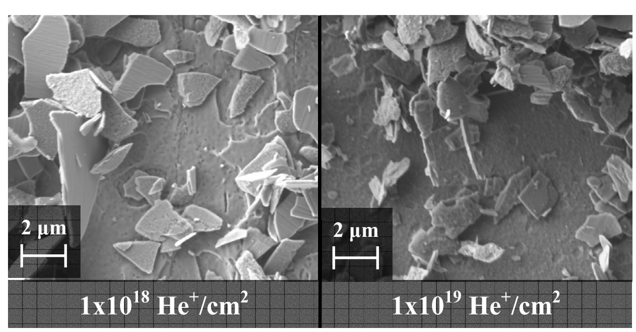

Figure 9. SiC Irradiated at 850 °C

are much larger in scale than individual flakes and might be caused by repeated flaking in those regions leaving the larger depressions.

IV.C. Masked SiC Sample Irradiated to 1×10^{19} He^{+}/cm^{2} at 950 °C

In addition to the previous experiments, a SiC specimen was partially masked by tantalum foil to segment the specimen into irradiated and unirradiated zones. A schematic of this masked configuration is shown below in Figure 11. This specific sample was irradiated to a fluence of 1×10^{19} He^{+}/cm^{2} and a temperature of 950 °C. The goal of this experiment was to determine whether the observed surface damage was a result of temperature exposure or ion fluence. SEM micrographs were taken in the center of both the irradiated region which experience ion flux and temperature exposure and also in the unirradiated region which experienced only the temperature exposure. It is clear from Figure 12 that the irradiated region has sustained substantial cratering and flaking due to energetic helium ion bombardment. The unirradiated region looks much like the virgin specimen shown in Figure 4. The small contaminants on the surface in the unirradiated region are believed to be post-irradiation artifacts occurring during the sample's removal from the IEC device and SEM imaging.

Finally, a comparison is made between the previous fusion materials experiments and the current research on SiC. Each of the presented samples was irradiated to 1×10^{19} He^{+}/cm^{2} and temperatures between 800 - 830 °C. The surface morphology changes of polycrystalline tungsten, tantalum carbide foam, and silicon carbide to energetic He^{+} bombardment are illustrated in Figure 13. One notices that the type of surface damage exhibited by these specimens varies significantly. In the tungsten pore formation is dominant and the damage is homogenous over the sample surface. Similarly, the tantalum carbide experiences this pore formation, which is also homogenous over the sample. The difference between the previous two materials and the silicon carbide is striking. One notices the damage effects are much larger scale and inhomogeneous. Cratering and flaking damage appears to be dominant, with pore formation secondary irradiation response.

V. DISCUSSION

Several relevant observations can be drawn from the range of experiments performed on the CVD SiC. It is evident that each of the fluences and irradiation temperatures investigated cause significant changes in the surface morphology of the SiC. These changes take the form of cratering, flaking, and pore formation, resultant from the energetic helium ion bombardment.

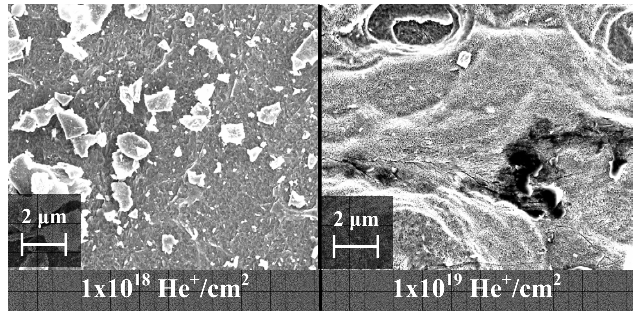

Figure 10. SiC Irradiated at 950 °C

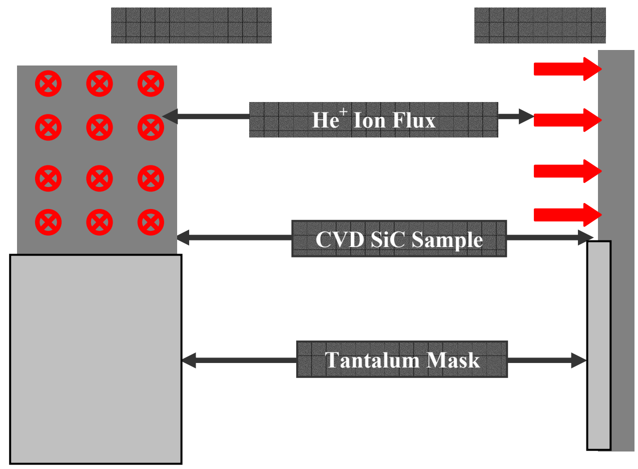

Figure 11. Schematic of Masked SiC Sample

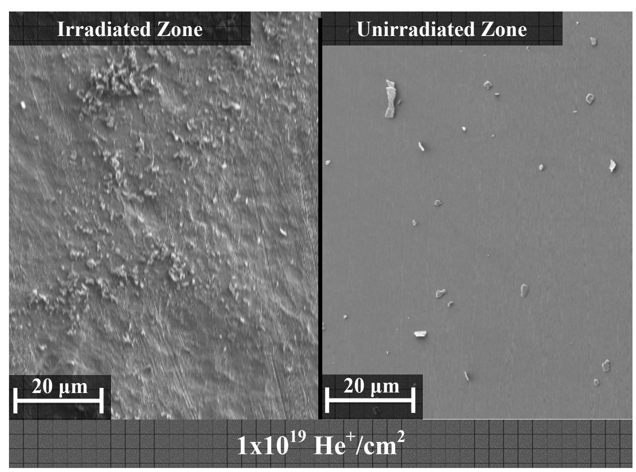

Figure 12. Masked Sample Reveals Surface Morphology Differences Between Irradiated and Unirradiated Regions

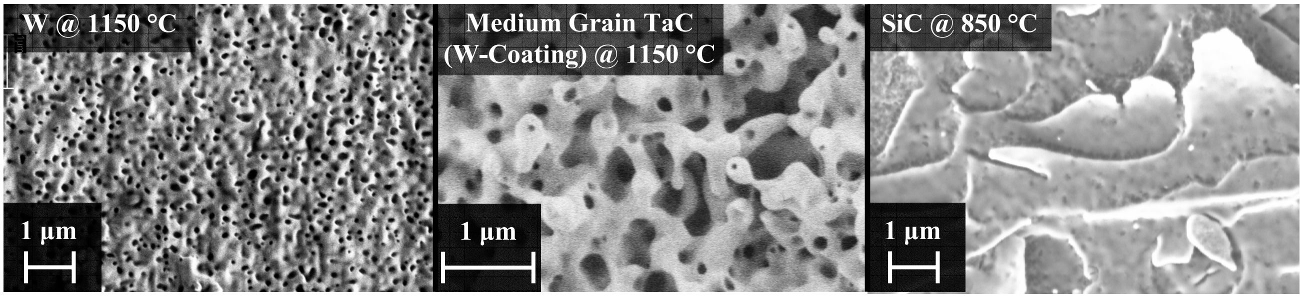

Figure 13. Comparison of Fusion Materials Irradiated to 1x10^{19} He$^+$/cm^2 using Energetic Helium Ions

As mentioned earlier, each sample appears to have sustained cratering. This cratering is most likely a result of repeated flaking of the sample surface. SRIM calculations estimating the range of the helium ions in SiC support this possibility. Some of the depressions observed in these various samples (~1 µm in depth) would require repeated flaking during irradiation, assuming the SRIM calculations have correctly predicted the helium ion range.

At constant fluence, data also shows that the type and extent of damage observed is a function of the temperature at which the sample is irradiated. Figure 7 is a clear illustration of this fact. Furthermore, it is ion bombardment, not temperature, which is the cause of the damage. Only after samples have been exposed to ion bombardment do we notice surface morphology changes. This conclusion is evident from the SEM micrographs of the masked SiC sample shown in Figure 12.

A final conclusion is that the damage mechanisms vary with different first wall choices. For different materials irradiated to the same fluences and similar temperatures metallic specimens appear to be dominated by pore formation. The silicon carbide experiences extensive cratering and flaking with less pore formation at similar conditions. One also notices that the polycrystalline tungsten and tantalum carbide foam experience homogenous damage over the sample,[2,5] while the silicon carbide experiences highly inhomogeneous damage exhibited by the congregation of flakes over the samples.

Each of these samples illustrates that significant damage is incurred from irradiation by energetic helium ions. In fact, none of these materials show sufficient robustness to be used as the first wall armor of the HAPL chamber. It must also be noted that these experiments do not encompass the entire energy spectrum of the ion bombardment but only a fraction of it. Due to this fact, other alternatives warrant investigation, such as magnetic intervention to deflect ions, increased Xe gas pressure in the chamber to stop energetic ions, liquid walls, and moving solid walls. Regardless of the final design of the HAPL chamber, these materials investigations are important to ensure the best possible material is chosen based on resistance to radiation damage and economic feasibility.

VI. ACKNOWLEDGEMENTS

The authors of this paper would like to thank the Greatbatch Foundation, the Grainger Foundation, the Naval Research Lab, the University of Wisconsin and the Department of Energy for financial support. We also want to acknowledge Dr. Lance Snead at ORNL for providing the samples for these experiments. Finally, we would like to thank Greg Piefer, Chris Seyfert, and Brian Egle for their assistance and support.

REFERENCES

[1] J. Perkins. To be published.

[2] R.F. Radel and G.L. Kulcinski, "Implantation of D and He in W-coated Refractory Carbides," FUSION SCIENCE AND TECHNOLOGY, 47 (4) Part 2 May 2005

[3] G.L. Kulcinski, "Near term commercial opportunities for long range fusion research," FUSION TECHNOLOGY, 30 (3): 411-421 Part 2A DEC 1996.

[4] J.F. Ziegler, J.P. Biersack and U. Littmark, "The Stopping and Range of Ions in Solids," Pergamon Press, New York, 1985.

[5] B.B. Cipiti and G.L. Kulcinski, "Helium and deuterium implantation in tungsten at elevated temperatures," *Journal of Nuclear Materials,* Vol. 347 (3) 298-306, December 2005.